Wireless Pers Commun
DOI 10.1007/s11277-011-0275-x

The Impact of Shadowing and the Severity of Fading on the First and Second Order Statistics of the Capacity of OSTBC MIMO Nakagami-Lognormal Channels

Gulzaib Rafiq · Matthias Pätzold

Abstract This article presents a thorough statistical analysis of the capacity of orthogonal space-time block coded (OSTBC) multiple-input multiple-output (MIMO) Nakagami-lognormal (NLN) channels. The NLN channel model allows to study the joint effects of fast fading and shadowing on the statistical properties of the channel capacity. We have derived exact analytical expressions for the probability density function (PDF), cumulative distribution function (CDF), level-crossing rate (LCR), and average duration of fades (ADF) of the capacity of MIMO NLN channels. It is observed that an increase in the MIMO dimension or a decrease in the severity of fading results in an increase in the mean channel capacity, while the variance of the channel capacity decreases. On the other hand, an increase in the shadowing standard deviation increases the spread of the channel capacity, however the shadowing effect has no influence on the mean channel capacity. We have also presented approximation results for the statistical properties of the channel capacity, obtained using the Gauss-Hermite integration method. It is observed that approximation results not only reduce the complexity, but also have a very good fitting with the exact results. The presented results are very useful and general because they provide the flexibility to study the impact of shadowing on the channel capacity under different fading conditions. Moreover, the effects of

The material in this paper is based on "On the Statistical Properties of the Capacity of OSTBC Nakagami-Lognormal MIMO Channels", by Gulzaib Rafiq and Matthias Pätzold which appeared in the proceedings of 4th IEEE International Conference on Signal Processing and Communication Systems, ICSPCS 2010, Gold Coast, Australia, December 2010. © 2010 IEEE.

Throughout this paper, we will refer to the MIMO dimension as $N_R \times N_T$, where N_R is the number of receive antennas and N_T denotes the number of transmit antennas.

G. Rafiq (✉) · M. Pätzold
Department of Information and Communication Technology, Faculty of Engineering and Science, University of Agder, Service box 509, 4898 Grimstad, Norway
e-mail: gulzaib.rafiq@uia.no

M. Pätzold
e-mail: matthias.paetzold@uia.no

Published online: 30 March 2011

severity of fading on the channel capacity can also be studied. The correctness of theoretical results is confirmed by simulations.

Keywords Nakagami-lognormal channels · MIMO · Land mobile terrestrial channels · Channel capacity · Shadowing effects · Level-crossing rate · Average duration of fades

1 Introduction

Multiple-input multiple-output (MIMO) systems exploit spatial diversity by utilizing multiple antennas at the receiver and transmitter in order to increase the spectral efficiency and to acquire a diversity gain [1]. To achieve the desired capacity in MIMO channels, space-time coding techniques, such as space-time trellis codes (STTC) [2] or space-time block codes (STBC) [3,4] are considered to be an effective method. Among different space-time coding techniques, OSTBC has gained much attention in recent years due to its orthogonal structure, which allows to use maximum likelihood decoding at the receiver [4]. Hence, it results in a decrease in the complexity of the receiver structure. Another advantage of using OSTBC is that it transforms MIMO fading channels into equivalent single-input single-output (SISO) channels, which significantly simplifies the mathematical formulation of MIMO channels [5]. Studies pertaining to the analysis of the capacity of OSTBC MIMO channels can be found in [6,7]. The outage performance and the error probability analysis of OSTBC MIMO systems have been studied in [8–10]. Moreover, the statistical properties of the capacity of OSTBC MIMO Nakagami-m channels have been analyzed in [11].

The analyses presented in the aforementioned articles only consider fast fading in MIMO channels due to multipath propagation, where the local mean of the received signal envelope is assumed to be constant [12]. While for land mobile terrestrial channels, the local mean fluctuates due to shadowing effects [13]. Moreover, shadowing can adequately be modelled by a lognormal process and can be incorporated in the channel model as a multiplicative process [13–16]. Hence, to study the joint effects of fast fading and shadowing in land mobile terrestrial channels, the Suzuki process is considered to be a more appropriate channel model [14]. A Suzuki process can be expressed as a product of a Rayleigh process and a lognormal process. However, by employing a Nakagami-m process instead of the Rayleigh process in a Suzuki process, we obtain a more general channel model referred to as the NLN channel model [15,16], which contains the Suzuki process as a special case when the Nakagami parameter $m = 1$. The generality of this model derives from the fact that the one-sided Gaussian and Rayleigh processes are inherently included in the Nakagami-m process as special cases, i.e., for $m = 0.5$ and $m = 1$, respectively. Moreover, it can be used to study the scenarios where the fading is more (or less) severe as compared to Rayleigh fading [17,18].

For MIMO channels, the authors in [19] have proposed a channel model that takes into account the joint effects of shadowing and fast fading. This model is then employed in [20] to study the outage performance in OSTBC MIMO channels. The analysis in [19] and [20] is however restricted only to MIMO Rayleigh channels. While in this article, we have considered a more general channel model referred to as MIMO NLN channel model, where the fast fading in the MIMO channel is modeled by a Nakagami-m process as compared to the Rayleigh process in [19]. Thereafter, we have analyzed the statistical properties of the capacity of MIMO NLN channels for the case when OSTBC is employed. To the best of the authors' knowledge, the statistical properties of the capacity of OSTBC MIMO NLN channels have not been investigated so far. The MIMO NLN channel model provides the

flexibility to study the impact of shadowing on the channel capacity under different fading conditions. Moreover, the effects of severity of fading on the channel capacity can also be studied.

This paper analyzes the statistical properties of the capacity of OSTBC MIMO NLN channels for various levels of shadowing and for different MIMO dimensions. We have derived exact analytical expressions for the PDF, CDF, LCR, and ADF of the capacity of MIMO NLN channels. The mean value and spread of the channel capacity has been analyzed with the help of the PDF of the channel capacity. On the other hand, the analysis of the LCR and ADF of the channel capacity is very helpful to study the temporal behavior of the channel capacity. It is observed that an increase in the MIMO dimension or a decrease in the severity of fading results in an increase in the mean channel capacity, while the variance of the channel capacity decreases. Moreover, the shadowing effect has no influence on the mean channel capacity, whereas an increase in the shadowing standard deviation increases the spread of the channel capacity. It is also observed that an increase in either the shadow standard deviation or the MIMO dimension decreases the maximum value of the LCR of the channel capacity. Whereas, this effect decreases the ADF of the channel capacity only at higher levels. We have also presented approximation results for the statistical properties of the channel capacity using the Gauss-Hermite integration method [21]. It is observed that the approximation results not only reduce the complexity, but also have a very good fitting with the exact results.

The remainder of this paper is organized as follows. In Sect. 2, we first give a brief description of the MIMO NLN channel model. Thereafter, the capacity of MIMO NLN channels is formulated for the case when OSTBC is employed. Section 3 presents the statistical properties of the capacity of OSTBC MIMO NLN channels. Section 4 deals with the analysis and illustration of the theoretical as well as the simulation results. Finally, the conclusions are drawn in Sect. 5.

2 The Capacity of OSTBC MIMO NLN Channels

In this article, we have considered a MIMO system with N_T transmit and N_R receive antennas. The input-output relation for such a system is given by

$$\mathbf{y}(t) = \hat{\mathbf{H}}(t)\mathbf{x}(t) + \mathbf{n}(t) \tag{1}$$

where $\mathbf{x}(t)$ is an $N_T \times 1$ transmit signal vector, $\mathbf{y}(t)$ is an $N_R \times 1$ received signal vector, $\hat{\mathbf{H}}(t)$ is the $N_R \times N_T$ channel matrix, and $\mathbf{n}(t)$ is an $N_R \times 1$ additive white Gaussian noise (AWGN) vector. In order to study the joint effects of fast fading and shadowing in MIMO channels, the authors in [19] have proposed the following MIMO channel model

$$\hat{\mathbf{H}}(t) = \lambda(t)\mathbf{H}(t) \tag{2}$$

where $\mathbf{H}(t)$ is the $N_R \times N_T$ matrix with complex random independent and identically distributed (i.i.d.) entries $h_{i,j}(t)$, which model the fast fading in the channel between the ith receive and jth transmit antenna. In addition to fast fading, it is assumed that the local mean of the signal envelope fluctuates due to shadowing. Moreover, shadowing can adequately be modelled by a lognormal process $\lambda(t)$ and can be incorporated in the channel model as a multiplicative process. Hence, the lognormal process $\lambda(t)$ is multiplied to $\mathbf{H}(t)$ in (2). Furthermore, shadowing influences the signal envelope on large spatial scales as compared to the fast fading, thus it is assumed that a single lognormal process $\lambda(t)$ equally effects all the elements of the matrix $\mathbf{H}(t)$ and is independent of $\mathbf{H}(t)$. In [19], the authors have restricted

the analysis to Rayleigh channels, where the envelope $\left|h_{i,j}(t)\right|$ is Rayleigh distributed. However, in this article, we have assumed that the envelope $\left|h_{i,j}(t)\right|$ of the complex entries $h_{i,j}(t)$ follows a Nakagami-m distribution given by

$$p_{|h_{i,j}(t)|}(r) = \frac{2m_{i,j}^{m_{i,j}} r^{2m_{i,j}-1}}{\Gamma\left(m_{i,j}\right)\Omega_{i,j}^{m_{i,j}}} e^{-\frac{m_{i,j}r^2}{\Omega_{i,j}}}, \quad r \geq 0 \tag{3}$$

where $\Omega_{i,j} = E\left\{|h_{i,j}(t)|^2\right\}$, $m_{i,j} = \Omega_{i,j}^2 \big/ \mathrm{Var}\left\{|h_{i,j}(t)|^2\right\}$, and $\Gamma(\cdot)$ represents the gamma function [22]. Here, $E\{\cdot\}$ and $\mathrm{Var}\{\cdot\}$ denote the mean (or the statistical expectation) and the variance operators, respectively. Moreover, the phase of the complex entries $h_{i,j}(t)$ is considered to be uniformly distributed between $[0, 2\pi)$. The lognormal process $\lambda(t)$ in (1) can be expressed as

$$\lambda(t) = 10^{[\sigma_L \nu(t) + m_L]/20} \tag{4}$$

where σ_L represents the shadowing standard deviation, m_L denotes the area mean, and $\nu(t)$ is a zero-mean real-valued Gaussian process with unit variance. The PDF $p_\lambda(z)$ of the lognormal process $\lambda(t)$ can be written as

$$p_\lambda(z) = \frac{20}{z\sigma_L\sqrt{2\pi}\ln(10)} e^{-\frac{(10\log(z)-m_L)^2}{2\sigma_L^2}}, \quad z \geq 0. \tag{5}$$

There exist numerous models in the literature for the spectral shape of the Gaussian process $\nu(t)$ in (4). In this article, we have assumed a Gaussian power spectral density (PSD) for the Gaussian process $\nu(t)$ given by [14,23]

$$S_{\nu\nu}(f) = \frac{1}{\sqrt{2\pi}\sigma_c} e^{-\frac{f^2}{2\sigma_c^2}} \tag{6}$$

where the parameter σ_c controls the spread of the PSD $S_{\nu\nu}(f)$ and can be expressed in terms of the 3 dB cutoff frequency f_c as $\sigma_c = f_c/\sqrt{2\ln(2)}$. We have assumed that the value of f_c is much smaller than the maximum Doppler frequency $f_{\max}$, i.e., $f_{\max}/f_c \gg 1$. By taking the inverse Fourier transform of $S_{\nu\nu}(f)$, the ACF $r_{\nu\nu}(\tau)$ of the process $\nu(t)$ can be expressed as

$$r_{\nu\nu}(\tau) = e^{-2(\pi\sigma_c\tau)^2}. \tag{7}$$

The capacity of OSTBC MIMO systems can be expressed as [24]

$$C(t) = \log_2\left(1 + \frac{\gamma_s}{N_T}\lambda^2(t)\mathbf{h}^H(t)\mathbf{h}(t)\right) \quad \text{(bits/s/Hz)} \tag{8}$$

where $\mathbf{h}(t)$ represents the $N_R N_T \times 1$ vector formed by stacking the columns of the $N_R \times N_T$ matrix $\mathbf{H}(t)$ one below the other. For simplicity, we will represent the entries of the vector $\mathbf{h}(t)$ as $h_i(t)$ $(i = 1, 2, \ldots, N_R N_T)$. It can clearly be seen that the envelopes $|h_i(t)|$ are i.i.d. following the Nakagami-m distribution in (3) with the parameters m_i and Ω_i. In (8), $(\cdot)^H$ denotes the Hermitian operator, and γ_s is the signal-to-noise ratio (SNR). In order to generate Nakagami-m processes $|h_i(t)|$, the following relation can be employed [18]

$$|h_i(t)| = \sqrt{\sum_{n=1}^{2m_i} \mu_{n,i}^2(t)} \tag{9}$$

where $\mu_{n,i}(t)$ $(n = 1, 2, \ldots, 2m_i)$ are the underlying i.i.d. Gaussian processes, and m_i is the parameter of the Nakagami-m distribution associated with the ith channel $h_i(t)$. The parameter m_i controls the severity of the fading. Increasing the value of m_i decreases the severity of fading associated with the ith channel $h_i(t)$ and vice versa. In this article, we have assumed that $\Omega_i = 2m_i\sigma_0^2$ for the sake of simplicity. Here, σ_0^2 denotes the variance of the underlying Gaussian processes $\mu_{n,i}(t)$ in $|h_i(t)|$. The channel capacity $C(t)$ given by (8) can be written as

$$\begin{aligned} C(t) &= \log_2\left(1 + \gamma_s'\lambda^2(t)\sum_{i=1}^{N_R N_T}\chi_i^2(t)\right) \text{ (bits/s/Hz)} \\ &= \log_2\left(1 + \gamma_s'\Xi(t)\right) \end{aligned} \tag{10}$$

where $\gamma_s' = \gamma_s \,/ N_T$, $\Xi(t) = \lambda^2(t)\sum_{i=1}^{N_R N_T}\chi_i^2(t)$, and $\chi_i^2(t) = |h_i(t)|^2$ $(i = 1, 2, \ldots, N_R N_T)$. Due to the assumption that the envelope $|h_i(t)|$ is Nakagami-m distributed, the squared envelope $\chi_i^2(t)$ follows the gamma distribution [25, Eq. (1)]. Let $Y(t) = \sum_{i=1}^{N_R N_T}\chi_i^2(t)$, then the PDF $p_\Xi(z)$ of $\Xi(t)$ can be expressed using [25, Eq. (2)], (5), and by employing the relationship $p_\Xi(z) = \int_{-\infty}^{\infty} 1 \,/ |y| \; p_Y(z/y)p_{\lambda^2}(y)dy$ [26] as

$$p_\Xi(z) = \frac{10z^{\acute{\alpha}-1}\beta^{-\acute{\alpha}}}{\sqrt{2\pi}\ln(10)\sigma_L\Gamma(\acute{\alpha})}\int_0^\infty \left(\frac{1}{y}\right)^{\acute{\alpha}+1} e^{-\frac{(10\log y - m_L)^2}{2\sigma_L^2}} e^{-\frac{z}{y\beta}}, z \geq 0 \tag{11}$$

where $\acute{\alpha} = \sum_{i=1}^{N_R N_T}\alpha_i$ and $\beta = \Omega_i \,/ m_i = 2\sigma_0^2$. In order to derive the expressions for the LCR of the OSTBC MIMO NLN channel capacity, we require the joint PDF $p_{\Xi\dot{\Xi}}(z, \dot{z})$ of $\Xi(t)$ and $\dot{\Xi}(t)$ at the same time t. In this article, the time derivative of a process is denoted by an overdot. The joint PDF $p_{\Xi\dot{\Xi}}(z, \dot{z})$ can be expressed using [14, Eq. (40)], [27, Eq. (35)], and with the help of the relationship $p_{\Xi\dot{\Xi}}(z, \dot{z}) = \int_0^\infty \int_{-\infty}^\infty 1 \,/ y^2 \; p_{Y\dot{Y}}(z/y, \dot{z}/y - \dot{y}z/y^2)p_{\lambda^2\dot{\lambda}^2}(y, \dot{y})d\dot{y}dy$ [28] as

$$\begin{aligned} p_{\Xi\dot{\Xi}}(z, \dot{z}) = {} & \frac{\left(5 \,/ 2\pi\right) z^{\acute{\alpha}-3/2}\beta^{-\acute{\alpha}}}{\ln(10)\sqrt{\beta_N}\sigma_L\Gamma(\acute{\alpha})}\int_0^\infty y^{-\acute{\alpha}-3/2}\frac{e^{-\frac{z}{y\beta}}}{K(z, y)} e^{-\frac{(10\log y - m_L)^2}{2\sigma_L^2}} e^{-\frac{\dot{z}^2}{8\beta_N zyK^2(z,y)}}, \\ & z \geq 0, |\dot{z}| < \infty \end{aligned} \tag{12a}$$

where

$$K(z, y) = \sqrt{1 + \frac{z\gamma\sigma_L^2}{y\beta_N(20 / \ln(10))^2}} \tag{12b}$$

and

$$\gamma = -\ddot{r}_{\nu\nu}(\tau)|_{\tau=0} = (2\pi\sigma_c)^2 . \tag{12c}$$

In (12a), $\beta_N = 2(\pi\sigma_0 f_{\max})^2$ for isotropic scattering conditions [27]. In the next section, we will derive the expressions for the PDF, CDF, LCR, and ADF of the capacity of OSTBC MIMO NLN channels.

3 Statistical Properties of the Capacity of OSTBC MIMO NLN Channels

The expression in (11) can be considered as a mapping of the random process $\Xi(t)$ to another random process $C(t)$. Hence, the statistical properties of the process $\Xi(t)$ can be used to find the statistical properties of the channel capacity. By applying the concept of transformation of random variables [26, Eq. (7–8)], the PDF $p_C(r)$ of the channel capacity $C(t)$ is obtained as follows

$$\begin{aligned} p_C(r) &= \frac{2^r \ln(2)}{\gamma_s'} p_\Xi\left(\frac{2^r-1}{\gamma_s'}\right) \\ &= \frac{10\ln(2) 2^r (2^r-1)^{\acute{\alpha}-1}}{(\gamma_s'\beta)^{\acute{\alpha}}\sqrt{2\pi}\ln(10)\sigma_L\Gamma(\acute{\alpha})} \int_0^\infty \left(\frac{1}{y}\right)^{\acute{\alpha}+1} e^{-\frac{2^r-1}{\gamma_s' y\beta}} e^{-\frac{(10\log y - m_L)^2}{2\sigma_L^2}} \end{aligned} \tag{13}$$

for $r \geq 0$. The CDF $F_C(r)$ of the channel capacity $C(t)$ can be found using the relationship $F_C(r) = \int_0^r p_C(x)dx$ [26]. After solving the integral, the CDF $F_C(r)$ of $C(t)$ can be expressed as

$$F_C(r) = 1 - \frac{10/\ln(10)}{\sqrt{2\pi}\sigma_L\beta^{\acute{\alpha}}\Gamma(\acute{\alpha})} \int_0^\infty \left(\frac{1}{y}\right)^{\acute{\alpha}+1} e^{-\frac{(10\log y - m_L)^2}{2\sigma_L^2}} \Gamma\left(\acute{\alpha}, \frac{2^r-1}{y\gamma_s'\beta}\right), \quad r \geq 0 \tag{14}$$

where $\Gamma(\cdot,\cdot)$ represents the incomplete gamma function [22, Eq. (8.350–2)].

The LCR of the channel capacity defines the average rate of up-crossings (or down-crossings) of the channel capacity through a certain threshold level [29]. In the literature, there exist numerous articles dealing with the analysis of the LCR of the received signal envelope and the channel capacity (see, e.g., [13,29–31], and the references therein). The analysis pertaining to the LCR of the received signal envelope has applications in the finite-state Markov modelling (FSMM) of fading channels [32], the analysis of handoff algorithms [33], and estimation of packet error rates [34]. In a similar fashion, using FSMM for the instantaneous capacity evolving process $C(t)$ and feeding the predicted capacity to the transmitter allows it to adapt the transmission rate according to the instantaneous channel capacity to minimize the probability of errors. For single-input single-output (SISO) channels, the LCR $N_C(r)$ of the channel capacity $C(t)$ can be expressed in terms of the LCR $N_X(r)$ of the received signal envelop $X(t)$ as $N_C(r) = N_X\left(\sqrt{(2^r-1)/\gamma_s'}\right)$ (see Appendix A for the proof). However in order to find the LCR $N_C(r)$ of the capacity $C(t)$ of MIMO channels, we first need to find the joint PDF $p_{C\dot{C}}(z,\dot{z})$ of the channel capacity $C(t)$ and its time derivative $\dot{C}(t)$. The joint PDF $p_{C\dot{C}}(z,\dot{z})$ can be obtained as

$$\begin{aligned} p_{C\dot{C}}(z,\dot{z}) &= \left(\frac{2^z\ln(2)}{\gamma_s'}\right)^2 p_{\Xi\dot{\Xi}}\left(\frac{2^z-1}{\gamma_s'}, \frac{2^z\dot{z}\ln(2)}{\gamma_s'}\right) \\ &= \frac{10\,(2^z\ln(2))^2\,(2^z-1)^{\acute{\alpha}-3/2}}{\sqrt{\gamma_s'\beta_N}4\pi\sigma_L\beta^{-\acute{\alpha}}\Gamma(\acute{\alpha})} \int_0^\infty y^{-\acute{\alpha}-3/2} \frac{e^{-\frac{2^z-1}{\gamma_s' y\beta}}}{K\left(\frac{2^z-1}{\gamma_s'}, y\right)} e^{-\frac{(10\log y - m_L)^2}{2\sigma_L^2}} \\ &\quad \times e^{-\frac{(2^z\ln(2)\dot{z})^2}{8\beta_N(2^z-1)\gamma_s' y K^2\left(\frac{2^z-1}{\gamma_s'}, y\right)}} dy \end{aligned} \tag{15}$$

for $z \geq 0$ and $|\dot{z}| < \infty$. The LCR $N_C(r)$ can now be obtained by solving the integral in $N_C(r) = \int_0^\infty \dot{z}\, p_{C\dot{C}}(r,\dot{z})d\dot{z}$. After some algebraic manipulations, the LCR $N_C(r)$ can finally be expressed as

$$N_C(r) = \frac{10\,(2^r-1)^{\acute{\alpha}-1/2}\sqrt{\gamma_s'\beta_N}}{(\gamma_s'\beta)^{\acute{\alpha}}\pi\,\ln(10)\sigma_L\Gamma(\acute{\alpha})}\int_0^{\infty}\left(\frac{1}{y}\right)^{\acute{\alpha}+1/2} e^{-\frac{2^r-1}{\gamma_s' y\beta}} K\left(\frac{2^z-1}{\gamma_s'}, y\right) \times e^{-\frac{(10\log y - m_L)^2}{2\sigma_L^2}}, \quad r \geq 0. \tag{16}$$

The ADF of the channel capacity denotes the average duration of time over which the channel capacity is below a certain threshold level [29]. The ADF $T_C(r)$ of the channel capacity $C(t)$ can be obtained using [12]

$$T_C(r) = \frac{F_C(r)}{N_C(r)} \tag{17}$$

where $F_C(r)$ and $N_C(r)$ are given by (11) and (13), respectively.

3.1 Approximation of the Statistical Properties of the Channel Capacity Using Gauss-Hermite Integration Method

By letting $(10\log y - m_L)^2 = 2\sigma_L^2 x^2$, we can express the Eqs. (13), (14), and (16) as

$$p_C(r) = \frac{2^r\ln(2)\,(2^r-1)^{\acute{\alpha}-1}}{(\gamma_s'\beta)^{\acute{\alpha}}\sqrt{\pi}\Gamma(\acute{\alpha})}\int_{-\infty}^{\infty} e^{-x^2} f_1(r,x)dx, \quad r \geq 0 \tag{18}$$

$$F_C(r) = \frac{1}{\sqrt{\pi}\beta^{\acute{\alpha}}\Gamma(\acute{\alpha})}\int_{-\infty}^{\infty} e^{-x^2} f_2(r,x)dx, \quad r \geq 0 \tag{19}$$

$$N_C(r) = \frac{(2^r-1)^{\acute{\alpha}-\frac{1}{2}}\sqrt{2\gamma_s'}}{(\gamma_s'\beta)^{\acute{\alpha}}\pi\Gamma(\acute{\alpha})/\sqrt{\beta_N}}\int_{-\infty}^{\infty} e^{-x^2} f_3(r,x)dx, \quad r \geq 0 \tag{20}$$

respectively, where $f_1(r,x)$, $f_2(r,x)$, and $f_3(r,x)$ are given by

$$f_1(r,x) = e^{\left(-\frac{2^r-1}{\gamma_s'\beta}\right)10^{-\frac{\sqrt{2}\sigma_L x+m_L}{10}}}\,10^{-\acute{\alpha}\left(\frac{\sqrt{2}\sigma_L x+m_L}{10}\right)} \tag{21}$$

$$f_2(r,x) = \Gamma\left(\acute{\alpha}, \frac{(2^r-1)/\gamma_s'\beta}{10^{\frac{\sqrt{2}\sigma_L x+m_L}{10}}}\right)10^{-\acute{\alpha}\left(\frac{\sqrt{2}\sigma_L x+m_L}{10}\right)} \tag{22}$$

$$f_3(r,x) = e^{\left(-\frac{2^r-1}{\gamma_s'\beta}\right)10^{-\frac{\sqrt{2}\sigma_L x+m_L}{10}}}\,10^{-\left(\acute{\alpha}-\frac{1}{2}\right)\left(\frac{\sqrt{2}\sigma_L x+m_L}{10}\right)} \times K\left(\frac{2^r-1}{\gamma_s'}, 10^{\frac{\sqrt{2}\sigma_L x+m_L}{10}}\right) \tag{23}$$

respectively. The integrals $I_i = \int_{-\infty}^{\infty} e^{-x^2} f_i(r,x)dx$ $(i = 1, 2, \text{and } 3)$ in (18)–(20) can now be approximated using the Gauss-Hermite integration method [21] as

$$I_i = \int_{-\infty}^{\infty} e^{-x^2} f_i(r,x)dx \approx \sum_{m=1}^{M} W_m f_i(r,\omega_m) \tag{24}$$

where ω_m, W_m, and M are the roots, weighting factors, and the order, respectively, of the Hermite polynomials $H_M(x) = (-1)^N e^{x^2}\, d^M/dx^M\left(e^{-x^2}\right)$. Here d^M/dx^M represents the Mth

order differentiation of the exponential function e^{-x^2} with respect to x. The approximation in (24) yields many advantages. Firstly, it allows to get rid of the cumbersome integrals in (18)–(20), which reduces the complexity of the results. Secondly, it is observed that using only a small number of the terms M in (24) provides a very good fitting with the exact results, specifically for Rayleigh-lognormal MIMO channels (i.e., for $m_i = 1$) with smaller dimensions (e.g., 2×2). Moreover, the values of the roots (ω_m) and weighting factors (W_m) for a given M are constant irrespective of the integrand $e^{-x^2} f_i(r, x)$ ($i = 1, 2$, and 3). The tables containing the values of ω_m and W_m can easily be found in literature (see, e.g., [35]), or can be obtained numerically using numerical computation softwares, such as MATLAB and MATHEMATICA.

4 Numerical Results

In this section, we will discuss the analytical results obtained in the previous section and their validity will be tested by simulations. In order to investigate the influence of shadowing on the capacity of OSTBC MIMO NLN channels, we have studied the results for different values of the shadowing standard deviation σ_L, ranging from 1 dB to 10 dB. Specifically, the results for $\sigma_L = 4.3$ dB (urban environment [36]) and $\sigma_L = 7.5$ dB (suburban environment [36]) are shown. For comparison purposes, we have included a special case, namely the OSTBC MIMO Nakagami-m channels ($\sigma_L \to 0$ dB). Moreover, we have also presented the approximation results for the statistical properties of the channel capacity given by (18)–(20) and (24). It is observed in all cases that the approximation results match the exact theoretical results very closely. Furthermore, we have also studied the impact of the MIMO dimension on the statistical properties of the channel capacity for both $\sigma_L = 4.3$ dB and $\sigma_L = 7.5$ dB.

The Nakagami-m distributed waveforms $|h_i(t)|$ ($i = 1, 2, \ldots, N_R N_T$) are generated using (9). In order to simulate Gaussian processes $\mu_{n,i}(t)$ ($n = 1, 2, \ldots, 2m_i$) and $\nu(t)$ in (9) and (4), respectively, we have employed the sum-of-sinusoids (SOS) model [30,38,39]. The motivation behind choosing an SOS-based channel simulator is that it is widely acknowledged for its simplicity in implementation, accuracy, and flexibility to simulate nearly all kinds of fading channels under isotropic scattering conditions [30]. The SOS model is based on the superposition principle stating that a superposition of infinitely large number of weighted harmonic wave forms results in a stochastic Gaussian process. The harmonic waveforms (sinusoids) are describe with the help of model parameters, namely the gains, frequencies, and phases. The performance of the SOS model is strongly dependent on the parameters computation method. We have employed an SOS model with constant gains, constant frequencies and random phases uniformly distributed over the interval $(0, 2\pi]$. To calculate the suitable values for the gains and frequencies, we have used the generalized method of exact Doppler spread (GMEDS_1) [37]. The GMEDS is considered to be an extremely efficient method for the generation of an unlimited number of uncorrelated Gaussian waveforms [37]. The number of sinusoids used for the generation of the Gaussian distributed waveforms was selected to be $N = 21$. The maximum Doppler frequency $f_{\max}$ was 91 Hz, the SNR γ_s was chosen to be 15 dB, and $\sigma_0^2 = 1$. Finally, using (2), (4), and (8), the simulation results for the statistical properties of the capacity $C(t)$ of OSTBC MIMO NLN channels were obtained using MATLAB.

Figures 1 and 2 present the PDF of the capacity of OSTBC MIMO NLN channels for different values of the shadowing standard deviation σ_L and for different MIMO dimensions,

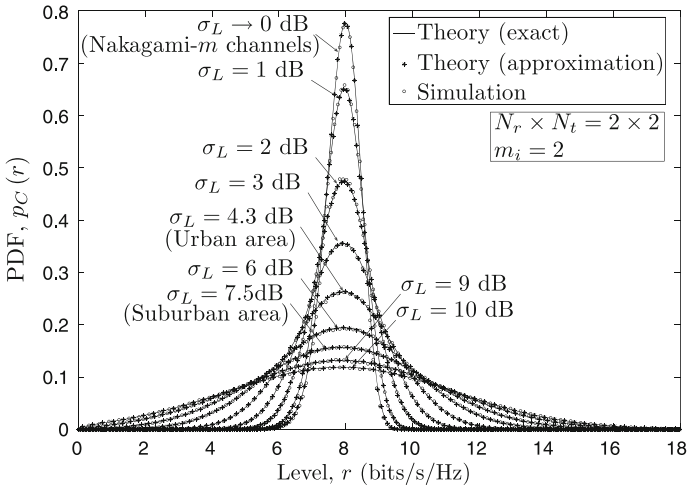

Fig. 1 The PDF $p_C(r)$ of the capacity $C(t)$ of OSTBC MIMO NLN channels for different values of the shadowing standard deviation σ_L

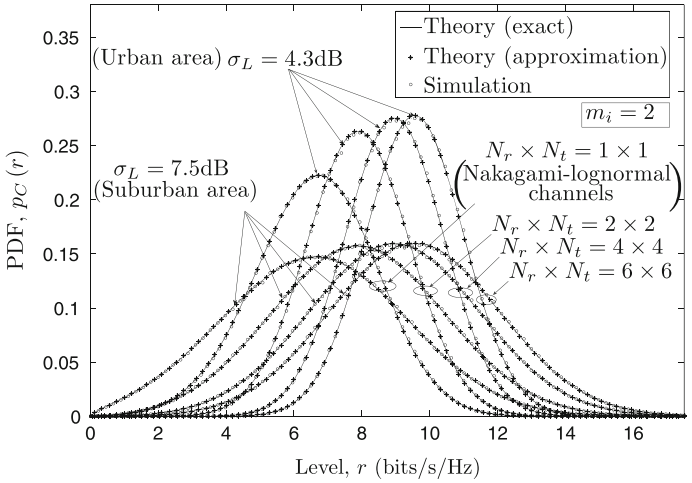

Fig. 2 The PDF $p_C(r)$ of the capacity $C(t)$ of OSTBC MIMO NLN channels for different MIMO dimensions

respectively. It is observed that an increase in the shadowing standard deviation σ_L increases the spread of the channel capacity, while it has no influence on the mean channel capacity. Moreover, an increase in the MIMO dimension results in an increase in the mean channel capacity, whereas the spread of the channel capacity decreases. This fact is specifically highlighted in Figs. 3 and 4, where the mean channel capacity and the variance of the channel capacity, respectively, are studied for different values of the shadowing standard deviation σ_L and for different MIMO dimensions. It can be observed that there is approximately a unit increase in the channel capacity when the MIMO dimension is increased from 2×2 to 4×4 (or from 4×4 to 6×6). In addition, the variance of the capacity of 2×2 MIMO systems with $\sigma_L = 10$ dB is almost 38 times the variance of the ones with $\sigma_L = 0$ dB. We have also analyzed the influence of severity of fading on the mean channel capacity and the variance

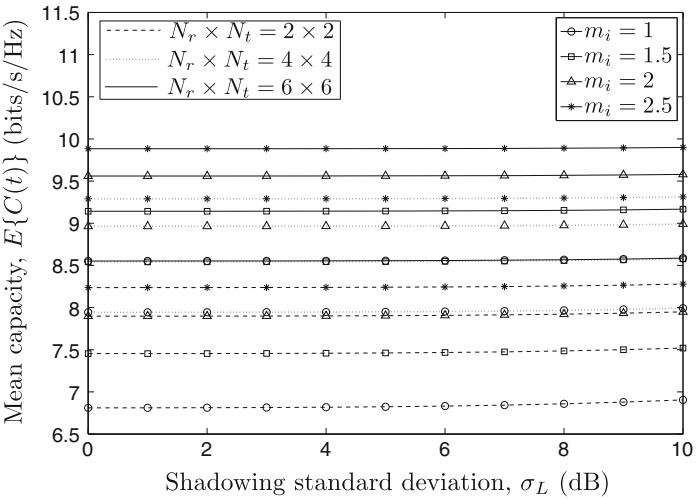

Fig. 3 The mean channel capacity $E\{C(t)\}$ of OSTBC MIMO NLN channels

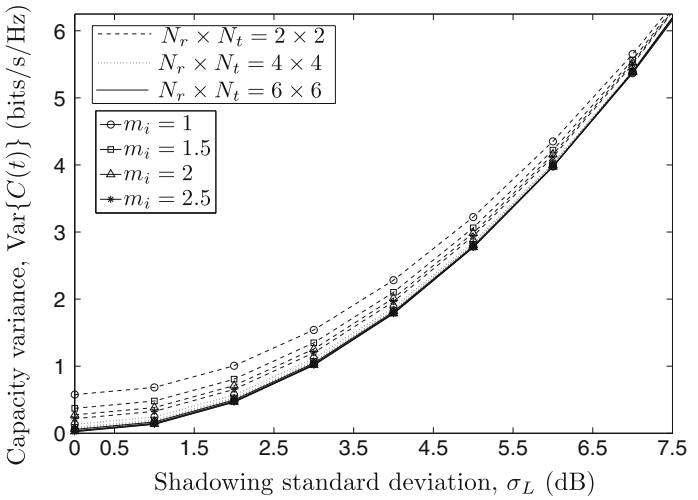

Fig. 4 The variance $\mathrm{Var}\{C(t)\}$ of the capacity of OSTBC MIMO NLN channels

of the channel capacity. The results show that as the fading severity increases, the mean channel capacity decreases. However, this effect has an opposite influence on the variance of the channel capacity. For the sake of completeness, we have also illustrated the CDF of the capacity of OSTBC MIMO NLN channels for different values of the shadowing standard deviation σ_L and for different MIMO dimensions in Figs. 5 and 6, respectively. The results presented in Figs. 5 and 6 can be studied to draw similar conclusions regarding the influence of shadowing standard deviation σ_L as well as the MIMO dimensions on the mean channel capacity and the variance of the channel capacity as from Figs. 1 and 2.

Figures 7 and 8 highlight the influence of shadowing and MIMO dimensions on the LCR of the channel capacity. It is observed that an increase in the shadowing standard deviation σ_L or the MIMO dimension results in a decrease in the maximum value of the LCR of the

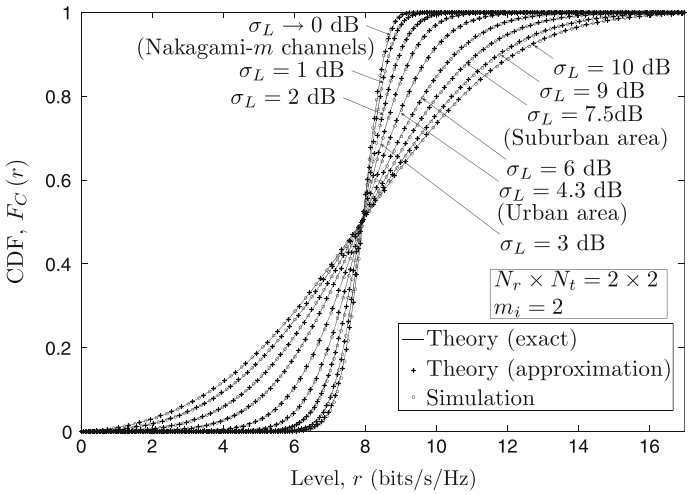

Fig. 5 The CDF $F_C(r)$ of the capacity $C(t)$ of OSTBC MIMO NLN channels for different values of the shadowing standard deviation σ_L

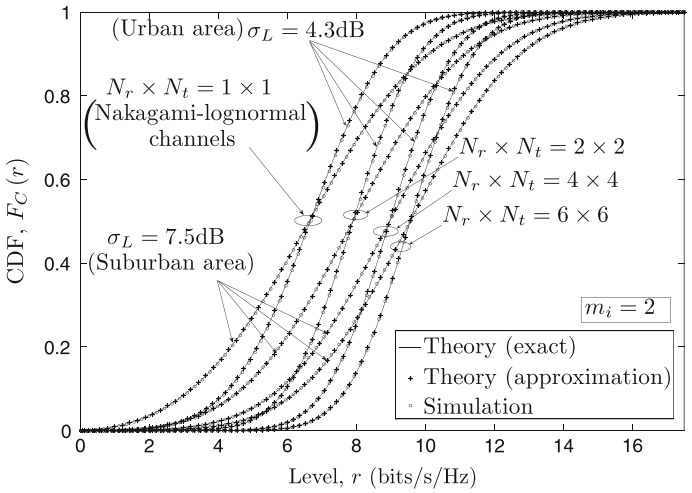

Fig. 6 The CDF $F_C(r)$ of the capacity $C(t)$ of OSTBC MIMO NLN channels for different MIMO dimensions

channel capacity, while the spread of the LCR increases. For example, for 2×2 MIMO systems with $m_i = 2$, an increase in the shadowing standard deviation σ_L from 0 to 10 dB decreases the maximum value of the LCR by a factor of 4.3. The results also show that at low and medium signal levels r, the channel capacity of systems with smaller MIMO dimensions has a higher LCR as compared to the ones with larger MIMO dimensions. The ADF of the channel capacity for different values of the shadowing standard deviation σ_L and for different MIMO dimensions is presented in Figs. 9 and 10, respectively. It is observed that at higher signal levels r, an increase in the shadowing standard deviation σ_L decreases the ADF of the channel capacity. However, the converse statement is true for lower signal levels. Moreover, an increase in the MIMO dimension has a similar influence on the ADF

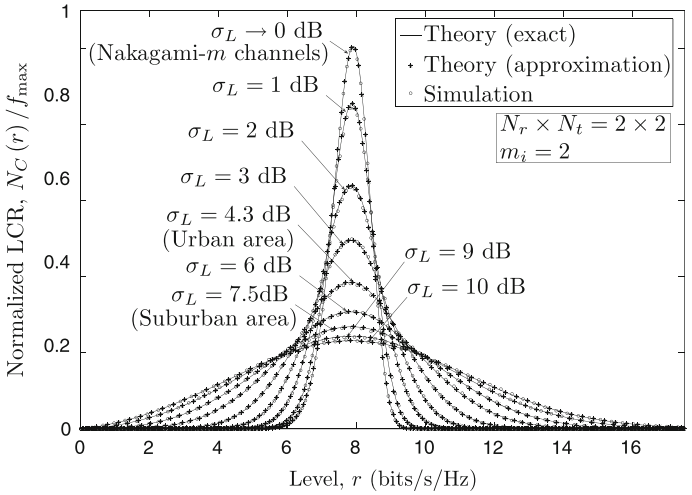

Fig. 7 The normalized LCR $N_C(r)/f_{\max}$ of the capacity $C(t)$ of OSTBC MIMO NLN channels for different values of the shadowing standard deviation σ_L

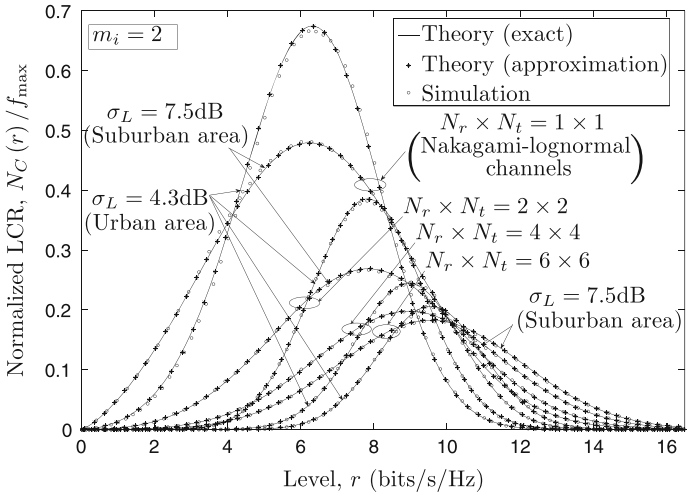

Fig. 8 The normalized LCR $N_C(r)/f_{\max}$ of the capacity $C(t)$ of OSTBC MIMO NLN channels for different MIMO dimensions

of the channel capacity as the shadowing standard deviation σ_L. Specifically, at a level of 5 bits/s/Hz, the ADF of the capacity of 2×2 MIMO systems with $\sigma_L = 10$ dB is 21 times higher than that of the systems with $\sigma_L = 0$ dB. The analytical expressions are verified using simulations, whereby an excellent fitting is observed.

5 Conclusion

This paper studies the statistical properties of the capacity of OSTBC MIMO NLN channels for various levels of shadowing and for different MIMO dimensions. We have derived

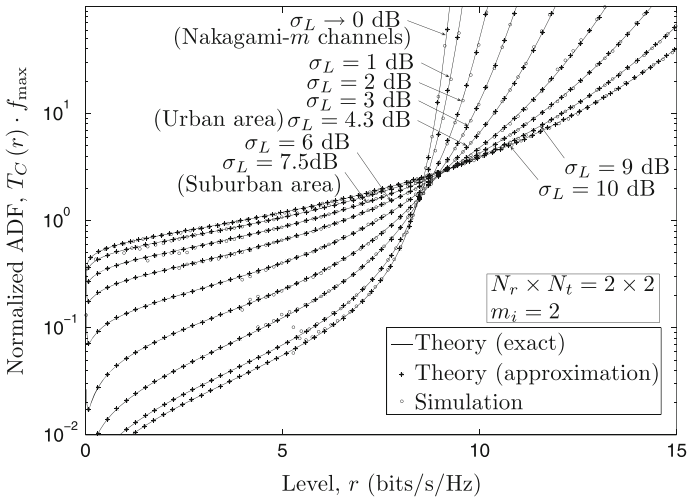

Fig. 9 The normalized ADF $T_C(r) \cdot f_{\max}$ of the capacity $C(t)$ of OSTBC MIMO NLN channels for different values of the shadowing standard deviation σ_L

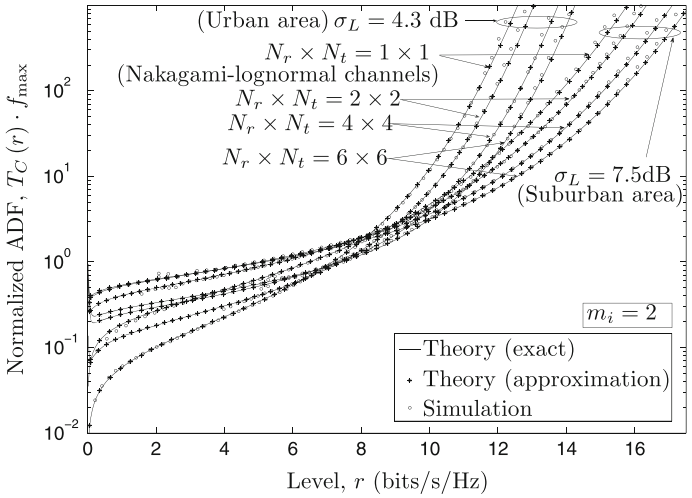

Fig. 10 The normalized ADF $T_C(r) \cdot f_{\max}$ of the capacity $C(t)$ of OSTBC MIMO NLN channels for different MIMO dimensions

exact analytical expressions for the PDF, CDF, LCR, and ADF of the capacity of MIMO NLN channels. It is observed that an increase in the MIMO dimension or a decrease in the severity of fading results in an increase in the mean channel capacity, while the variance of the channel capacity decreases. On the other hand, the shadowing effect has no influence on the mean channel capacity; however an increase in the shadowing standard deviation increases the spread of the channel capacity. It is also observed that an increase in either the shadow standard deviation or the MIMO dimension decreases the maximum value of the LCR of the channel capacity. Whereas, this effect decreases the ADF of the channel capacity only at higher signal levels. We have also presented approximation results for the statistical

properties of the channel capacity obtained using the Gauss-Hermite integration method. It is observed that the approximation results reduce the complexity as well as fit very closely to the exact results. The correctness of the analytical results is confirmed by simulations.

A Appendix

Consider the received signal envelop in a SISO system denoted by $X(t)$. The corresponding channel capacity can be expressed as $C(t) = \log_2\left(1 + \gamma_s X^2(t)\right)$, where γ_s denotes the average received SNR. The LCR $N_C(r)$ of the channel capacity $C(t)$ is defined as [29]

$$N_C(r) = \int_0^\infty \dot{z}\, p_{C\dot{C}}(r, \dot{z})\, d\dot{z}, \quad r \geq 0 \tag{5.1}$$

where $p_{C\dot{C}}(z, \dot{z})$ denotes the joint PDF of $C(t)$ and $\dot{C}(t)$. By applying the concept of transformation of random variables [26, Eqs. (7–8)], the joint PDF $p_{C\dot{C}}(z, \dot{z})$ can be obtained using $p_{C\dot{C}}(z, \dot{z}) = \left(2^z \ln(2) \big/ \gamma_s\right)^2 p_{X^2\dot{X}^2}\left((2^z - 1) \big/ \gamma_s,\, (2^z \dot{z} \ln(2)) \big/ \gamma_s\right)$, where $p_{X^2\dot{X}^2}(z, \dot{z}) = \left(1 \big/ (4z)\right) p_{X\dot{X}}\left(\sqrt{z}, \dot{z} \big/ (2\sqrt{z})\right)$.

By substituting $p_{C\dot{C}}(z, \dot{z})$ in (5.1) and letting $\dot{w} = (2^z \dot{z} \ln(2)\sqrt{\gamma_s}) \big/ (2\sqrt{2^z - 1})$, the LCR $N_C(r)$ can be finally expressed as

$$N_C(r) = \int_0^\infty \dot{w}\, p_{X\dot{X}}\left(\sqrt{\frac{2^r - 1}{\gamma_s}}, \dot{w}\right) d\dot{w} = N_X\left(\sqrt{\frac{2^r - 1}{\gamma_s}}\right) \tag{5.2}$$

where $N_X(r)$ is the LCR of the received signal envelope $X(t)$ [38,39].

References

1. Zheng, L., & Tse, D. N. C. (2003). Diversity and multiplexing: A fundamental tradeoff in multiple antenna channels. *IEEE Transactions on Information Theory, 49*, 1073–1096.
2. Tarokh, V., Seshadri, N., & Calderbank, A. R. (1998). Space-time codes for high data rate wireless communication: Performance criterion and code construction. *IEEE Transactions on Information Theory, 44*(2), 744–765.
3. Alamouti, S. M. (1998). A simple transmit diversity technique for wireless communications. *IEEE Journal on Selected Areas in Communications, 16*(8), 1451–1458.
4. Tarokh, V., Jafarkhani, H., & Calderbank, A. R. (1999). Space-time block codes from orthogonal designs. *IEEE Transactions on Information Theory, 45*(5), 1456–1467.
5. Larsson, E. G., & Stoica, P. (2003). *Space-time block coding for wireless communications* (1st ed.). New York, NY: Cambridge University Press.
6. Chen, J., Du, Z., & Gao, X. (2008). Approximate capacity of OSTBC-OFDM in spatially correlated MIMO Nakagami-*m* fading channels. *Electronics Letters, 44*(8), 534–535.
7. Musavian, L., Dohler, M., Nakhai, M. R., & Aghvami, M. H. (2004). Closed-form capacity expressions of orthogonalized correlated MIMO channels. *IEEE Communications Letters, 8*(6), 365–367.
8. Yang, L. (2008). Outage performance of OSTBC in double scattering MIMO channels. *Wireless Personal Communications, 45*(2), 225–230.
9. Zhang, H., & Gulliver, T. A. (2005). Capacity and error probability analysis for orthogonal space-time block codes over fading channels. *IEEE Transaction on Wireless Communications, 4*(2), 808–819.
10. Maaref, A., & Aïssa, S. (2006). Performance analysis of orthogonal space-time block codes in spatially correlated MIMO Nakagami fading channels. *IEEE Transaction on Wireless Communications, 5*(4), 807–817.

11. Rafiq, G., Pätzold, M., & Kontorovich, V. (2009). The influence of spatial correlation and severity of fading on the statistical properties of the capacity of OSTBC Nakagami-m MIMO channels. In *Proceedings IEEE 69th vehicular technology conference, IEEE VTC 2009-Spring*. Barcelona, Spain.
12. Jakes, W. C. (Ed.). (1994). *Microwave mobile communications*. Piscataway, NJ: IEEE Press.
13. Stüber, G. L. (2001). *Principles of mobile communications* (2nd ed.). Boston, MA: Kluwer Academic Publishers.
14. Pätzold, M., Killat, U., & Laue, F. (1998). An extended Suzuki model for land mobile satellite channels and its statistical properties. *IEEE Transactions on Vehicular Technology, 47*(2), 617–630.
15. Tjhung, T. T., & Chai, C. C. (1999). Fade statistics in Nakagami-lognormal channels. *IEEE Transactions on Communications, 47*(12), 1769–1772.
16. Ramos, F., Kontorovitch, V. Y., & Lara, M. (2000). Generalization of Suzuki model for analog communication channels. In *Proceedings IEEE antennas and propagation for wireless communication, IEEE APS 2000* (pp. 107–110).
17. Nakagami, M. (1960). The *m*-distribution: A general formula of intensity distribution of rapid fading. In W. G. Hoffman (Ed.), *Statistical methods in radio wave propagation*. Oxford, UK: Pergamon Press.
18. Yacoub, M. D., Vargas, J. E. B., & Guedes, L. G. R.de (1999). On higher order statistics of the Nakagami-*m* distribution. *IEEE Transactions on Vehicular Technology, 48*(3), 790–794.
19. Shen, Z., Heath, R. W., Jr., Andrews, J. G., & Evans, B. L. (2006). Space-time water-filling for composite MIMO fading channels. *EURASIP Journal on Wireless Communications and Networking, 2006*(2), 48–48.
20. Yang, L. (2007). Outage performance of OSTBC in MIMO channels with shadowing. *Wireless Personal Communications, 43*(4), 1751–1754.
21. Salzer, H. E., Zucker, R., & Capuano, R. (1952). Table of the zeros and weight factors of the first twenty hermite polynomials. *Journal of Research of the National Bureau of Standards, 48*, 111–116.
22. Gradshteyn, I. S., & Ryzhik, I. M. (2000). *Table of integrals, series, and products* (6th ed.). New York: Academic Press.
23. Pätzold, M., & Yang, K. (2006). An exact solution for the level-crossing rate of shadow fading processes modelled by using the sum-of-sinusoids principle. In *Proceedings 9th international symposium on wireless personal multimedia communications, WPMC 2006* (pp. 188–193). San Diego, USA.
24. Paulraj, A. J., Nabar, R., & Gore, D. (2003). *Introduction to space-time wireless communications*. Cambridge, UK: Cambridge University Press.
25. Alouini, M.-S., Abdi, A., & Kaveh, M. (2001). Sum of gamma variates and performance of wireless communication systems over Nakagami-fading channels. *IEEE Transactions on Vehicular Technology, 50*(6), 1471–1480.
26. Papoulis, A., & Pillai, S. U. (2002). *Probability, random variables and stochastic processes* (4th ed.). New York: McGraw-Hill.
27. Yacoub, M. D., da Silva, C. R. C. M., & Vargas Bautista, J. E. (2001). Second-order statistics for diversity-combining techniques in Nakagami-fading channels. *IEEE Transactions on Vehicular Technology, 50*(6), 1464–1470.
28. Krantzik, A., & Wolf, D. (1990). Distribution of the fading-intervals of modified Suzuki processes. In L. Torres, E. Masgrau, & M. A. Lagunas (Eds.), *Signal processing V: Theories and applications* (pp. 361–364). Amsterdam, The Netherlands: Elsevier Science Publishers, B.V.
29. Hogstad, B. O., & Pätzold, M. (2007). Exact closed-form expressions for the distribution, level-crossing rate, and average duration of fades of the capacity of MIMO channels. In *Proceedings 65th semiannual vehicular technology conference, IEEE VTC 2007-Spring* (pp. 455–460). Dublin, Ireland.
30. Pätzold, M. (2002). *Mobile fading channels*. Chichester: John Wiley & Sons.
31. Giorgetti, A., Smith, P. J., Shafi, M., & Chiani, M. (2003). MIMO capacity, level crossing rates and fades: The impact of spatial/temporal channel correlation. *Journal of Communications and Networks, 5*(2), 104–115.
32. Wang, H. S., & Moayeri, N. (1995). Finite-state Markov channel—a useful model for radio communication channels. *IEEE Transactions on Vehicular Technology, 44*(1), 163–171.
33. Vijayan, R., & Holtzman, J. M. (1993). Foundations for level crossing analysis of handoff algorithms. In *Proceedings IEEE international conference on communications, ICC 1993* (pp. 935–939). Geneva, Switzerland.
34. Lai, J., & Mandayam, N. B. (1998). Packet error rate for burst-error-correcting codes in Rayleigh fading channels. In *Proceedings of the IEEE 48th vehicular technology conference, VTC'98*. Ottawa, Ontario, Canada.
35. Abramowitz, M., & Stegun, I. A. (1984). *Handbook of mathematical functions with formulas, graphs, and mathematical tables*. Washington: National Bureau of Standards.

36. Gudmundson, M. (1991). Correlation model for shadow fading in mobile radio systems. *Electronics Letters, 27*(23), 2145–2146.
37. Pätzold, M., Wang, C. X., & Hogstad, B. O. (2009). Two new sum-of-sinusoids-based methods for the efficient generation of multiple uncorrelated Rayleigh fading waveforms. *IEEE Transactions on Wireless Communications, 8*(6), 3122–3131.
38. Rice, S. O. (1944). Mathematical analysis of random noise. *Bell System Technical Journal, 23*, 282–332.
39. Rice, S. O. (1945). Mathematical analysis of random noise. *Bell System Technical Journal, 24*, 46–156.

Author Biographies

Gulzaib Rafiq was born in Hyderabad, Pakistan, in 1982. He received his bachelor's degree (B.E.) in Electrical Engineering (E.E.) in 2003 from the National University of Engineering Sciences and Technology (NUST) in Rawalpindi, Pakistan, and his master's degree (M.S.) in Electronics Engineering in 2006 from Ghulam Ishaq Khan Institute of Engineering Sciences and Technology (GIK) in Topi, Pakistan. He was awarded gold medals in both B.E. and M.S. for the best final year project of E.E. department in 2003 and for securing first position in the academic session 2004–2006, respectively. His publications received one best paper award and one best poster presentation award. Since January 2007, he has been working on his Ph.D. thesis supervised by Professor Matthias Pätzold at the University of Agder in Grimstad, Norway. His current research interests include mobile fading channel modelling and information theoretic analysis of MIMO systems.

Matthias Pätzold received the Dipl.-Ing. and Dr.-Ing. degrees in electrical engineering from Ruhr-University Bochum, Bochum, Germany, in 1985 and 1989, respectively, and the habil. degree in communications engineering from the Technical University of Hamburg-Harburg, Hamburg, Germany, in 1998. From 1990 to 1992, he was with ANT Nachrichtentechnik GmbH, Backnang, Germany, where he was engaged in digital satellite communications. From 1992 to 2001, he was with the department of digital networks at the Technical University Hamburg-Harburg. Since 2001, he has been a full professor of mobile communications with the University of Agder, Norway. He authored several books and numerous technical papers. His publications received five best paper awards. He has been actively participating in numerous conferences serving as TPC chair and TPC member for more than 10 conferences within the recent 3–4 years.